Available online at www.sciencedirect.com

ScienceDirect

Procedia CIRP 45 (2016) 131 – 134

www.elsevier.com/locate/procedia

3rd CIRP Conference on Surface Integrity (CIRP CSI)

# Effect of process parameters on the surface roughness of overhanging structures in laser powder bed fusion additive manufacturing

Jason C. Fox[a]*, Shawn P. Moylan[a], Brandon M. Lane[a]

[a]*National Institute of Standards and Technology, 100 Bureau Drive, Gaithersburg, MD 20886, USA*

* Corresponding author. Tel.: +1-301-975-2171 ; fax: +1-301-975-8058. *E-mail address:* jason.fox@nist.gov

**Abstract**

The development of additive manufacturing has allowed for increased flexibility and complexity of designs over formative and subtractive manufacturing. However, a limiting factor of additive manufacturing is the as-built surface quality as well as the difficulty in maintaining an acceptable surface roughness in overhanging structures. In order to optimize surface roughness in these structures, samples covering a range of overhang angles and process parameters were built in a laser powder bed fusion system. Analysis of the surface roughness was then performed to determine a relationship between process parameters, angle of the overhanging surface, and surface roughness. It was found that the analysis of surface roughness metrics, such as *Rpc*, *Rsm*, and *Rc*, can indicate a shift between surfaces dominated by partially melted powder particles and surfaces dominated by material from the re-solidified melt track.



Peer-review under responsibility of the scientific committee of the 3rd CIRP Conference on Surface Integrity (CIRP CSI)
Keywords: Selective Laser Melting (SLM); Roughness; Overhangs

## 1. Introduction

Additive manufacturing (AM) is a layer by layer process that fabricates parts directly from a 3-D digital model. This is accomplished by slicing the model into layers to create 2-D cross sections that the equipment can use as build instructions. Laser Powder Bed Fusion (L-PBF), for example, will fabricate a part by spreading a thin layer of powder (20 µm to 100 µm) across a build platform and using a high power laser to selectively melt regions of that layer. Once the layer is melted, the build platform lowers, new powder is spread across the build platform, and the process repeats until the build is complete.

A key advantage to AM over formative (e.g., casting) or subtractive (e.g., milling) methods is the ability to produce highly complex shapes. However, a limiting factor in AM is the as-built quality of surfaces. Methods exist to process surfaces after a part has been built [1,2] and during the build process through laser re-melting [3] and pulse shaping [4], but as the complexity of parts increases, the ability to successfully post-process the surface decreases [5]. As such, the as-built surface quality of a part has been cited as a key need for AM [6].

The surface roughness of AM parts has been the focus of several studies. Mumtaz and Hopkinson performed a full factorial analysis of the top and side surface roughness of multilayer thin-wall Inconel 625 parts, finding that parameter changes that tend to decrease roughness on one surface increase it on the other and optimization of the surface roughness requires a thorough understanding of how changes in process parameters affect different aspects of the part [7]. Strano *et al.* investigated the effect of surface angle on roughness for upward-facing surfaces in 316L steel [8]. Diatlov analysed parts with a wide range of surface slopes and found potential for analysis of the spectrum of the surface profile parameter *Ra* to determine surface characteristics [9]. Jamshidinia and Kovacevic found that an increase in heat accumulated during the build of thin-walled structures increases the surface roughness through an increase in adherence of partially melted powder particles to the part surface [10].

Triantaphyllou *et al.* investigated the upward- and downward-facing surface roughness for varying angles, compared results from multiple measurement instruments, and found that the *Ssk* parameter can be used for differentiating between upward- and downward-facing surfaces [11]. Aside


Peer-review under responsibility of the scientific committee of the 3rd CIRP Conference on Surface Integrity (CIRP CSI)
doi:10.1016/j.procir.2016.02.347

from this, however, little research has been performed to characterize downward-facing surface roughness, which is often the highest roughness [12]. Additionally, there is a lack of understanding of how and when structures that characterize the surface occur and how they affect the measured surface roughness parameters.

There is a wide range of mechanisms that contributes to the roughness of an AM surface, including both the process input parameters as well as the complex physical processes that occur during melting and solidification of the metal powder [13]. Understanding of surface characteristics is required in determining their effects on fatigue properties and in designing parts with improved performance [6]. Additionally, surface roughness has the potential to be used as a process signature. A strong quantitative understanding of relationships between measured surface parameters and the surface characteristic causing variation in measurements can determine if defects stem from AM system condition and performance or necessary maintenance (such as beam focus adjustments).

The purpose of this research is to understand the relationship between surface roughness parameters and the contributing surface features as a function of beam power, travel velocity, and overhang angle.

## 2. Experimental procedure

Experiments were performed on the EOS M270[1] system at the National Institute of Standards and Technology (NIST) using the commercially available EOS StainlessSteel GP1 (corresponds to US classification 17-4 [14]). It should be noted that the material used for the build was powder reclaimed from prior builds using an 80 µm sieve. It is assumed that the condition of the powder can have a large effect on the surface quality of parts being built and analysis of the powder is currently underway. All parts were fabricated during the same build. Thus, while the specific details of the powder have not yet been determined, the powder conditions are consistent across all of the samples.

The parts were designed as parallelepipeds with varying angles of overhang (α) to determine the effect of overhang angle on the surface roughness of the downward-facing surface. Fig. 1 shows an example model of the parallelepiped with a 60˚ angle overhang (α = 60˚). Analysis was performed on overhang angles of 30˚, 45˚, 60˚, and 75˚ as measured from the build plane. Prior experience has shown that the 30˚ overhang would build poorly (or crash the build) if it were built without supporting structures. To avoid this problem, hatched supports were added beneath the overhang. A 1 mm wide strip down the centre of the overhanging surface was left unsupported to allow measurement of the as-built surface.

To assess the effect of process parameters on surface characteristics, contour parameters with varying beam power and travel velocity were chosen in order to cover a wide range of the process space. Selection of process parameters can be seen in Table 1.

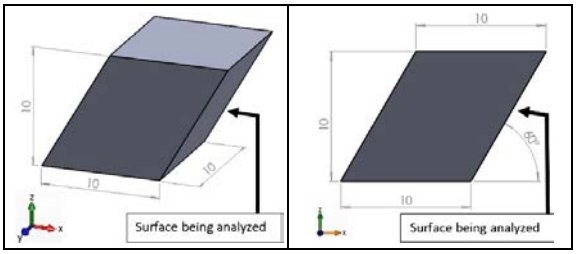


Fig. 1. Model parallelepiped for surface characterization, where α=60°. Dimensions are in millimeters. Build direction is positive z.

Table 1. Process parameters for experiments.

| Line Energy - *P/v* (J/m) | Power (W) | Velocity (mm/s) | Contour Number |
|---|---|---|---|
| 13.3 | 40 | 3000 | 1 |
| 35.7 | 25 | 700 | 2 |
| 46.7 | 140 | 3000 | 3 |
| 57.1 | 40 | 700 | 4 |
| 65 | 195 | 3000 | 5 |
| 71.4 | 25 | 350 | 6 |
| 114.3 | 40 | 350 | 7 |
| 116.4 | 195 | 1675 | 8 |
| 278.6 | 195 | 700 | 9 |

For each contour parameter set, parallelepipeds for each angle were built creating a total of 36 samples. To minimize the effect of incident angle of the laser beam and positional dependency on the build platform [15], all samples were positioned equidistant from the center of the build platform with the down-facing surface forming a straight line to the center of the beam source.

## 3. Analysis methods

Surface characterization was performed using a white light interferometer, described in detail in [16], and 10x objective lens. Using white light interferometry to analyze a very rough surface is a challenge due to difficulty in achieving null fringe condition (perfect leveling of the sample surface being measured). Because of this, a diamond-turned aluminum disk was first used to level the sample platform prior to any measurements. Thus, leveling the surface was performed as best as possible assuming that the surface being measured and the surface laying on the platform are parallel. This leveling procedure was performed before each measurement session to maintain a consistent leveling for each sample and prevent deviations due to errors caused by the leveling of the samples.

To create a large enough measurement of the sample surface to properly perform digital Gaussian filtering based on the ISO 4287 standard [17], nine images with 20 percent overlap were taken vertically down the downward-facing surface (in the build direction) and stitched together to create an

[1] Certain commercial entities, equipment, or materials may be identified in this document in order to describe an experimental procedure or concept adequately. Such identification is not intended to imply recommendation or endorsement by the National Institute of Standards and Technology, nor is it intended to imply that the entities, materials, or equipment are necessarily the best available for the purpose.

approximately 8 mm long measurement. The values presented used a bandpass digital Gaussian filter with a short cut-off length of 25 µm and a long cut-off length of 0.8 mm. The filtering process results in an evaluation length equal to five long cut-off lengths, or 4 mm. These filters are defined by ISO 4287 and represent a common practice in AM surface roughness research [18].

Scanning electron microscope (SEM) images were also taken for qualitative analysis of select surfaces.

## 4. Results

### *4.1. Qualitative Analysis*

SEM images for two of the α = 60˚ samples can be seen in Fig. 2. Fig. 2a) shows the downward-facing surface of the sample built with contour parameter set 4 and Fig. 2b) shows the downward-facing surface of the sample built with contour parameter set 9. From these images there is a clear difference in the structures that characterize the surface. In Fig. 2a) the surface is dominated by the adherence of partially melted powder particles, between which the solidified material of the part can be seen. In Fig. 2b) the adherence of partially melted powder particles is less prevalent and more of the solidified material of the part can be seen.

Material that has been deformed by the recoater blade (the mechanism for spreading powder across the build area) can be seen in Fig. 2b). The increased power that is being used for contour parameter set 9 could be creating several factors that result in the part impacting the recoater blade. Residual stress can cause the part to warp into the path of the recoater blade. An increase in the height of consolidated material, as seen by Yasa *et al.* [19] and Yadroitsev and Smurov [20], can be above the height of the new layer. Additionally, impact with the recoater blade could be caused by a combination of these two (or other) factors.

The challenge is to determine surface parameters that can discern these varying features.

### *4.2. Quantitative Analysis*

Analysis of *Ra* values can be seen in Fig. 3, which shows a clear dependence of surface angle on *Ra*. As α decreases, the value of *Ra* increases, which is expected and consistent with previous results [11]. However, it is also expected that the parametric analysis presented in this research would contain a relationship to *Ra* and a clear connection has not yet emerged. The results seen in Fig. 3 show that there is not a clear dependency on process parameters. Although not presented, this was also true of *Rq*, *Rz*, *Rt*, *Rp*, *RΔq*, and *Rsk*. Additional qualitative analysis to determine specific surface features caused by changes in process parameters is required to determine a relationship between process parameters and roughness parameters.

While the increase in *Ra* with decreasing α is an expected result, *Ra* does not yet provide a quantitative understanding of the specific surface characteristics seen in the qualitative analysis. One characteristic, however, can be seen in the analysis of *Rpc*, *RSm*, and *Rc* (peak count, mean width of profile elements, and mean height of profile elements, respectively). Seen in Fig. 4, as α decreases, *Rpc* decreases while *RSm* and *Rc* increase, suggesting that the number of peaks decrease but their overall size increases. Based on this result and the qualitative analysis of the surfaces, these changes are indicative of a shift between surfaces dominated by partially melted powder particles (seen at higher values of α or lower powers) and surfaces dominated by material from the re-solidified melt track (seen at lower values of α or higher powers). This result can also be seen in the SEM images presented in Fig. 2 and the respective values of *Rpc*, *RSm*, and *Rc*.

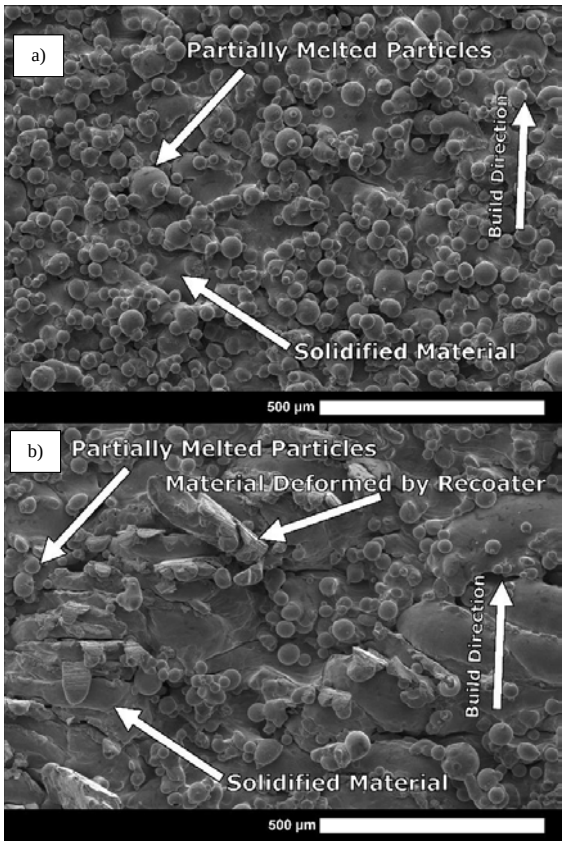


Fig. 2. SEM images of the downward-facing surface of the α=60˚samples built with a) contour parameter set 4 and b) contour parameter set 9.

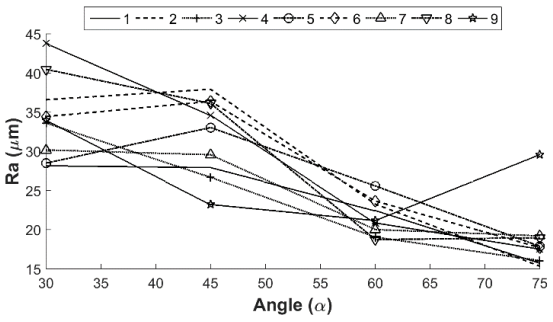


Fig. 3. *Ra* vs α for each contour parameter set.

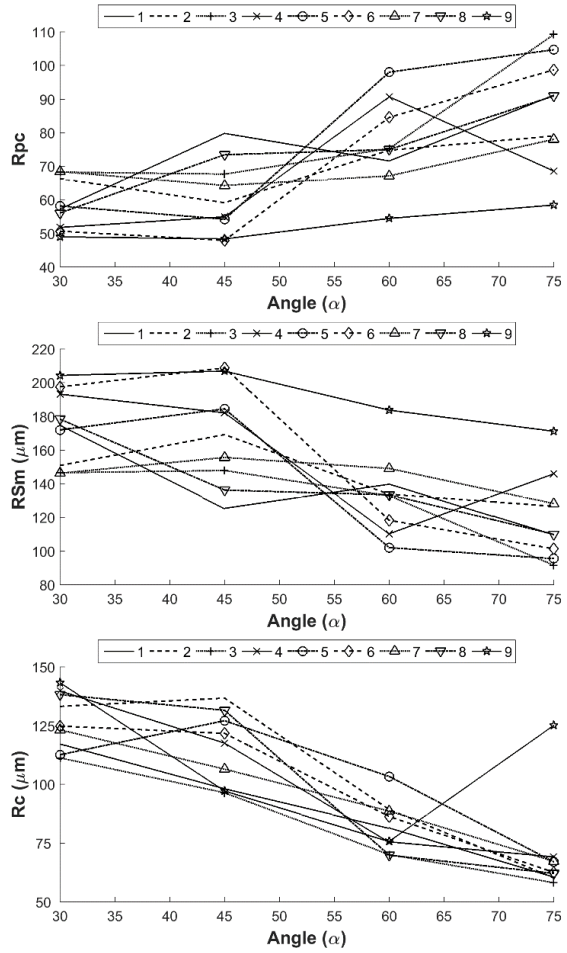


Fig. 4 *Rpc* (top), *RSm* (middle), and *Rc* (bottom) vs. α for each contour parameter set.

## 5. Conclusions

Analysis of the effect of beam power, beam velocity, and overhang angle has been presented to further the understanding of the relationship between individual surface characteristics and surface roughness parameters. It was found that the analysis of *Rpc*, *RSm*, and *Rc* can indicate a shift between surfaces dominated by partially melted powder particles (seen at higher values of α or lower powers) and surfaces dominated by material from the re-solidified melt track (seen at lower values of α or higher powers).

Analysis of process parameters on *Ra* did not show a distinct correlation, however, and it is suggested that further qualitative analysis of the individual features contributing to surface roughness will help these correlations emerge and will be the focus of future work.

## Acknowledgements

The authors would like to thank Dr. Mark Stoudt and Dr. Maureen Williams for their assistance taking SEM images.

## References

[1] Liu, X., Chu, P. K., and Ding, C., 2004, “Surface modification of titanium, titanium alloys, and related materials for biomedical applications,” Materials Science and Engineering: R: Reports, **47**(3–4), pp. 49–121. DOI: 10.1016/j.mser.2004.11.001.

[2] Lane, B. M., Moylan, S. P., and Whitenton, E. P., 2015, “Post-Process Machining of Additive Manufactured Stainless Steel,” Proceedings of the 2015 ASPE Spring Topical Meeting: Achieving Precision Tolerances in Additive Manufacturing, ASPE, Raleigh, NC.

[3] Yasa, E., Kruth, J.-P., and Deckers, J., 2011, “Manufacturing by combining Selective Laser Melting and Selective Laser Erosion/laser re-melting,” CIRP Annals - Manufacturing Technology, **60**(1), pp. 263–266. DOI: 10.1016/j.cirp.2011.03.063.

[4] Mumtaz, K. A., and Hopkinson, N., 2010, “Selective Laser Melting of thin wall parts using pulse shaping,” Journal of Materials Processing Technology, **210**(2), pp. 279–287. DOI: 10.1016/j.jmatprotec.2009.09.011.

[5] Pyka, G., Burakowski, A., Kerckhofs, G., Moesen, M., Van Bael, S., Schrooten, J., and Wevers, M., 2012, “Surface modification of Ti6Al4V open porous structures produced by additive manufacturing,” Adv. Eng. Mater., **14**(6), pp. 363–370. DOI: 10.1002/adem.201100344.

[6] 2012, “Measurement Science Roadmap for Metal-Based Additive Manufacturing,” National Institute of Standards and Technology, Gaithersburg, MD.

[7] Kamran Mumtaz, and Neil Hopkinson, 2009, “Top surface and side roughness of Inconel 625 parts processed using selective laser melting,” Rapid Prototyping Journal, **15**(2), pp. 96–103. DOI: 10.1108/13552540910943397.

[8] Strano, G., Hao, L., Everson, R. M., and Evans, K. E., 2013, “Surface roughness analysis, modelling and prediction in selective laser melting,” Journal of Materials Processing Technology, **213**(4), pp. 589–597. DOI: 10.1016/j.jmatprotec.2012.11.011.

[9] Diatlov, A., Buchbinder, D., Meiners, W., Wissenbach, K., and Bultmann, J., 2012, “Towards surface topography: Quantification of Selective Laser Melting (SLM) built parts,” Innovative Developments in Virtual and Physical Prototyping: Proceedings of the 5th International Conference on Advanced Research in Virtual and Rapid Prototyping, Taylor and Francis Inc., Leiria, Portugal, pp. 595–602.

[10] Jamshidinia, M., and Kovacevic, R., 2015, “The influence of heat accumulation on the surface roughness in powder-bed additive manufacturing,” Surf. Topogr.: Metrol. Prop., **3**(1), p. 014003. DOI: 10.1088/2051-672X/3/1/014003.

[11] Triantaphyllou, A., Giusca, C. L., Macaulay, G. D., Roerig, F., Hoebel, M., Leach, R. K., Tomita, B., and Milne, K. A., 2015, “Surface texture measurement for additive manufacturing,” Surf. Topogr.: Metrol. Prop., **3**(2), p. 024002. DOI: 10.1088/2051-672X/3/2/024002.

[12] Vandenbroucke, B., and Kruth, J.-P., 2007, “Selective laser melting of biocompatible metals for rapid manufacturing of medical parts,” Rapid Prototyping Journal, **13**(4), pp. 196–203.

[13] Taylor, J. S., 2015, “Physical processes linking input parameters and surface morphology in additive manufacturing,” Proceedings of the 2015 ASPE Spring Topical Meeting: Achieving Precision Tolerances in Additive Manufacturing, ASPE, Raleigh, NC, pp. 70–71.

[14] “Material data sheet - EOS StainlessSteel GP1” [Online]. Available: https://scrivito-public-cdn.s3-eu-west-1.amazonaws.com/eos/public/5f84f5d2c88ac900/05fb1582834a38c85ef6dd859733a230/EOS_StainlessSteel-GP1_en.pdf. [Accessed: 07-Dec-2015].

[15] Kleszczynski, S., Ladewig, A., Friedberger, K., zur Jacobsmühlen, J., Merhof, D., and Witt, G., “Position Dependency of Surface Roughness in Parts from Laser Beam Melting Systems.”

[16] Leach, R. K., ed., 2010, Fundamental Principles of Engineering Nanometrology, William Andrew Publishing, Oxford.

[17] ISO 4287:1997, 1997, Geometrical Product Specifications (GPS) – Surface texture: Profile method – Terms, definitions and surface texture parameters, ISO, Geneva.

[18] Petzing, J., Coupland, J., Leach, R. K., 2010, “The Measurement of Rough Surface Topography using Coherence Scanning Interferometry”, National Physical Laboratory Good practice guide No. 116, Teddington, UK.

[19] Yasa, E., Deckers, J., Craeghs, T., Badrossamay, M., and Kruth, J.-P., 2009, “Investigation on occurrence of elevated edges in selective laser melting,” International Solid Freeform Fabrication Symposium, Austin, TX, USA, pp. 673–85.

[20] Yadroitsev, I., and Smurov, I., 2011, “Surface Morphology in Selective Laser Melting of Metal Powders,” Physics Procedia, **12, Part A**, pp. 264–270. DOI: 10.1016/j.phpro.2011.03.034.